AN ABSTRACT OF THE THESIS OF

B. Ravindranath Baliga for the degree of Master of Ocean Engineering

in Civil Engineering presented on May 8, 1978.

Title: SAND WAVES IN A PRISTINE ESTUARY

Redacted for Privacy

Abstract approved:

Dr. Robert T. Hudspeth

The stochastic and the Fourier theories for sand waves developed by Lee(11) and Hino(6), respectively, for unidirectional flows are extended in order to estimate the rate of sediment turnover(RST) under oscillatory flows in the South Slough estuary, Coos Bay, Oregon. Data were collected by a mechanical and a sonic profiler. Histograms are given for the distributions of the elevations of deposition and erosion for sand wave data measured by the mechanical profiler. It may be observed from these distributions that the Gaussian assumption required for the application of the stochastic theory is not satisfied. The parameters for the step length distribution are estimated for only one elevation of deposition and erosion and the theoretical Gamma distribution is computed. Wave number amplitude spectra are estimated from the sonic profiler sand wave data. The maximum amplitude in the sand waves which were measured in the South Slough estuary lie in the fundamental harmonic component; while for the Coos Bay main channel, the spectral amplitudes for the sand waves are dispersed over a wider band of wave numbers. Due to the weak hydrodynamic influence, the sand waves in the South Slough estuary are still in the initial stage of their growth and it may not be possible to estimate RST in the South Slough estuary by the stochastic method outlined by Lee(11). Due to the strong tidal influence and/or ship disturbances, the sand wave spectral amplitudes are well dispersed for the Coos Bay main channel data and it is possible to estimate the RST in the main channel from a wave number spectrum using a transformation between wave numbers and wave frequencies.

Sand Waves in a Pristine Estuary

by

B. Ravindranath Baliga

A THESIS

submitted to

Oregon State University

in partial fulfillment of
the requirements for the
degree of

Master of Ocean Engineering

Completed May 8, 1978

Commencement June 1979

APPROVED:

Redacted for Privacy

Professor of Civil Engineering
in charge of major

Redacted for Privacy

Head of Department of Civil Engineering

Redacted for Privacy

Dean of Graduate School

Date thesis is presented May 8, 1978

Typed by B. Ravindranath Baliga

ACKNOWLEDGEMENTS

The support and guidance of Dr. R. T. Hudspeth is gratefully acknowledged in the research and writing of this thesis. The assistance of Dr. Carl Nordin, U. S. Geological Survey, Department of the Interior, in obtaining the sonic profiler is greatly appreciated. The suggestions from Dr. C. K. Sollitt, Dept. Civil Engineering, Dr. G. Alexander, Dept. Electrical Engineering and Dr. D. Solmon, Dept. Mathematics are accepted in gratitude.

The research was supported by the National Science Foundation under grant No. ENV71-01908.

TABLE OF CONTENTS

1.0 INTRODUCTION..... 1
1.1 Motivation..... 1
1.2 Past Application..... 2

2.0 STOCHASTIC ANALYSIS..... 6
2.1 Step Length Distribution..... 6
2.2 Rest Period Distribution..... 9

3.0 FOURIER ANALYSIS..... 12
3.1 Wave Number Spectrum..... 12
3.2 Wave Frequency Spectrum..... 13

4.0 DATA COLLECTION..... 17
4.1 Experimental Apparatus..... 17

5.0 DATA ANALYSES..... 23
5.1 Stochastic Analysis..... 23
5.2 Fourier Analysis..... 23

6.0 SUMMARY AND CONCLUSIONS..... 36
6.1 Stochastic Analysis..... 36
6.2 Fourier Analysis..... 38

REFERENCES..... 41

APPENDICES

I Derivation of "-3 power law" for wave number spectrum for sand waves..... 43
II Flow Chart for Estimating RST from wave number spectrum by Dispersion Transformation..... 45
III An Additional Method for Estimating RST..... 46

List of Symbols

$A_{yy}(\cdot)$ = spectral amplitude function for the sand wave profile;

C = celerity of sand wave;

d = diameter of the sand particle;

$E[\cdot|\cdot]$ = estimate of the conditional mean;

f = sand wave frequency;

f_1, f_∞ = lower and upper frequency bounds within the equilibrium subrange;

f_o = lowest frequency in the equilibrium subrange;

f_m = peak frequency of the wave frequency spectrum;

$f(\Psi)$ = a function of Ψ;

$f_{\bar{T}|Y_D}(t|y')$ = Gamma probability density distribution for conditional rest periods;

$f_{X|Y_E,Y_D}(x|y,y')$ = Gamma probability density distribution for conditional step lengths;

$H_{r.m.s}$ = root mean square wave height;

h = depth of water in channel;

$I_{(0,\infty)}(\cdot)$ = indicator function;

i = erosion;

j = deposition;

k = wave number;

k_o = smallest wave number in the equilibrium subrange;

k_m = peak wave number of the wave number spectrum;

l = number of dunes;

L = length of the sand wave record;

L_m = mode of the step length distribution;

L = wave length of a sand wave;

$m_{i,j}$ = total number of bed forms in the spatial sand wave record;

$m_{j,j}$ = total number of bed forms in the temporal sand wave record;

N = total number of digitizing values;

r_1 = shape parameter for the step length distribution;

r_2 = shape parameter for the rest period distribution;

List of Symbols(continued)

$S_{yy}(\cdot)$ = spectral density function for the sand wave profile;

T = total time of the sand wave record;

$\bar{T}$ = random variable for the rest period of the sand wave;

T_m = mode of the rest period distribution;

T = wave period of a sand wave;

t = argument for the random variable $\bar{T}$;

$t_{j,l}$ = rest period of the sand wave;

V = variance of the sand wave spectrum;

$Var[\cdot|\cdot]$ = estimate of the conditional variance;

V_* = shear velocity;

X = random variable for the step length of the sand wave;

x = argument for the random variable X;

$x_{i,j,l}$ = step length of the sand wave;

Y_D = random variable for the elevation of deposition;

Y_E = random variable for the elevation of erosion;

Y_{SD} = standardized elevation of deposition;

Y_{SE} = standardized elevation of erosion;

$Y_{SD\ MAX}$ = maximum standardized elevation of deposition;

$Y_{SE\ MAX}$ = maximum standardized elevation of erosion;

$Y_{SD\ MIN}$ = minimum standardized elevation of deposition;

$Y_{SE\ MIN}$ = minimum standardized elevation of erosion;

y, y' = arguments for the random variables, Y_E, Y_D, respectively;

y_i = elevation of erosion in the sample of sand wave record;

y_j = elevation of deposition in the sample of sand wave record;

$y_x(t)$ = temporal elevation of the sand wave profile for fixed x;

$y_t(x)$ = spatial elevation of the sand wave profile for fixed t;

$\alpha(\phi)$ = a function of ϕ;

β = drag coefficient;

List of symbols(continued)

γ = a constant of proportionality;

$\Gamma(\cdot)$ = Gamma function;

Δk = equal discrete wave number interval;

Δt = equal discrete time interval;

Δx = equal discrete spatial interval;

ΔY_{SD} = class interval for the standardized elevation of deposition;

ΔY_{SE} = class interval for the standardized elevation of erosion;

Δy = class interval for the standardized elevations of deposition and erosion;

κ_1 = scale parameter for the step length distribution;

κ_2 = scale parameter for the rest period distribution;

ρ_s = density of sand particles;

ρ_w = density of water;

ϕ = angle of repose of a sand particle;

Ψ = a nondimensional quantity related to the critical tractive force of the sand bed.

τ = shear stress at the sand bed; and

ω = velocity of water in a channel.

List of Figures and Tables

Figure		Page
1.	Location of sand wave sampling Stations in Coos Bay, Oregon estuary	3
2.	Typical $y_t(x)$ record for the Step length of a bed-load particle { cf. Lee(11)}	7
3.	Typical $y_x(t)$ record illustrating the conditional rest periods of a particle { cf. Lee(11)}	10
4.	Schematic of the Mechanical Sand Wave Profiler in place	18
5.	Histograms of the standardized elevations of deposition/erosion for record AB-I from a mechanical profiler	24
6.	Conditional Step Length Distribution for Record AB-I	26
7.	Sand wave amplitude spectrum for Record No. 1	30
8.	Sand wave amplitude spectrum for Record No. 3	31
9.	Sand wave amplitude spectrum for Record No. 4	32
10.	Sand wave amplitude spectrum for Record No. 5	33
11.	Sand wave amplitude spectrum for Record No. 6	34
12.	Sand wave amplitude spectrum for Record No. 7	35

Table		
1.	Summary of Data from Mechanical Profiler	19
2.	Summary of Data from Sonic Profiler	22
3.	Scale and Shape parameters of Gamma density function for conditional step length distribution for Record AB-I	25

SAND WAVES IN A PRISTINE ESTUARY

1.0 INTRODUCTION

1.1 Motivation

One of the objectives in the Oregon State University NSF-RANN study on environmental impacts of dredging was to develop a relation between the rate of sediment turnover(RST) and the organic content of the sediment(OCS). The NSF-RANN study on dredging was initiated because of the strong public interest in environmental concerns during the early 1970's. Contours of measures of various physical and biological properties of an estuarine ecosystem may be plotted on a dissection plane with RST and OCS as the axes. From these contours of this dissection plane, the impacts on the estuarine properties may be estimated from known or predicted alterations in the RST and OCS. Alterations in the RST may be observed due to the direct influence of the hydrodynamic forces on sand waves at the benthic interface of an estuary. Hence, sand waves subjected to hydrodynamic forces in an estuary were observed in order to estimate the rate of sediment turnover in a pristine estuary.

The hydrodynamic forces which directly influence the rate of sediment turnover at an erodible sediment interface result in an alternating sequence of erosion and deposition process. In those instances when this alternating sequence of erosion and deposition result in "wave like" deformation of the sediment boundary, wave propagation theories may be employed to compute the speed(C), wave length(L), and wave period(T) of these waves. In deterministic wave propagation problems, the reciprocal of the interval of periodicity yields the frequency(f) at which the process is repeated and provides an estimate of the RST. Since the benthic interfaces in most estuaries are far from sinusoidal or strictly periodic, the superposition of many waves may be employed to Fourier analyze the random interface. Also, the hydraulic processes which result in erosion and deposition are not, in general, deterministic and the methods of Fourier analyses must be further extended to describe a stochastic process.

In order to estimate the RST in an estuary by the migration of sand waves, the South Slough estuary, Coos Bay, Oregon was selected. Coos Bay, Oregon, is located on the southern Oregon Coast approximately 341 km south of the Columbia river entrance and 702 km north of San Francisco Bay. Fig. 1 shows the location of the estuary.

1.2 Past Application

The evolution of the various complex analytical models which describe the response of a deformable bottom to hydrodynamic forces is eloquently chronicled by Graf(5), by Raudkivi(14), and by Kennedy(7, 8). This evolution follows essentially the same three conceptual areas described by Kinsman(9) for random surface gravity waves; *viz.*, hydrodynamics, stochastic processes and probability, and Fourier analysis. The evolution of the hydrodynamic concept began with Exner{ cf Graf(5)} who assumed that the bottom was initially a sinusoid and that the free surface of the water was sensibly horizontal. Exner's model is capable(at least theoretically) of including the effects of friction in a channel of variable width. The principal contribution of this model is that the profile of the bed form results in a faster speed for the crest of the sinusoid compared to the trough and provides a means for estimating an approximate time for this sinusoid to become unstable and to collapse. Experimental verification of this model is lacking as well as a physical explanation of how the bed initially becomes a sinusoid and what shape it assumes following the instability of breaking.

Others(2,4,10,13,16) have extended this model to include a steady flow over a sinusoidal bottom with a sinusoidal free surface. The linearized potential theory solution derived by these authors yields a disturbing singularity for the special case when the speed of the free surface sinusoidal profile is exactly equal to the free stream velocity. The existence of this singularity is frequently used to argue that a deformable bedform may not remain flat. Kennedy(7,8) and Reynolds (15) also included a slowly moving sinusoidal bottom in their model.

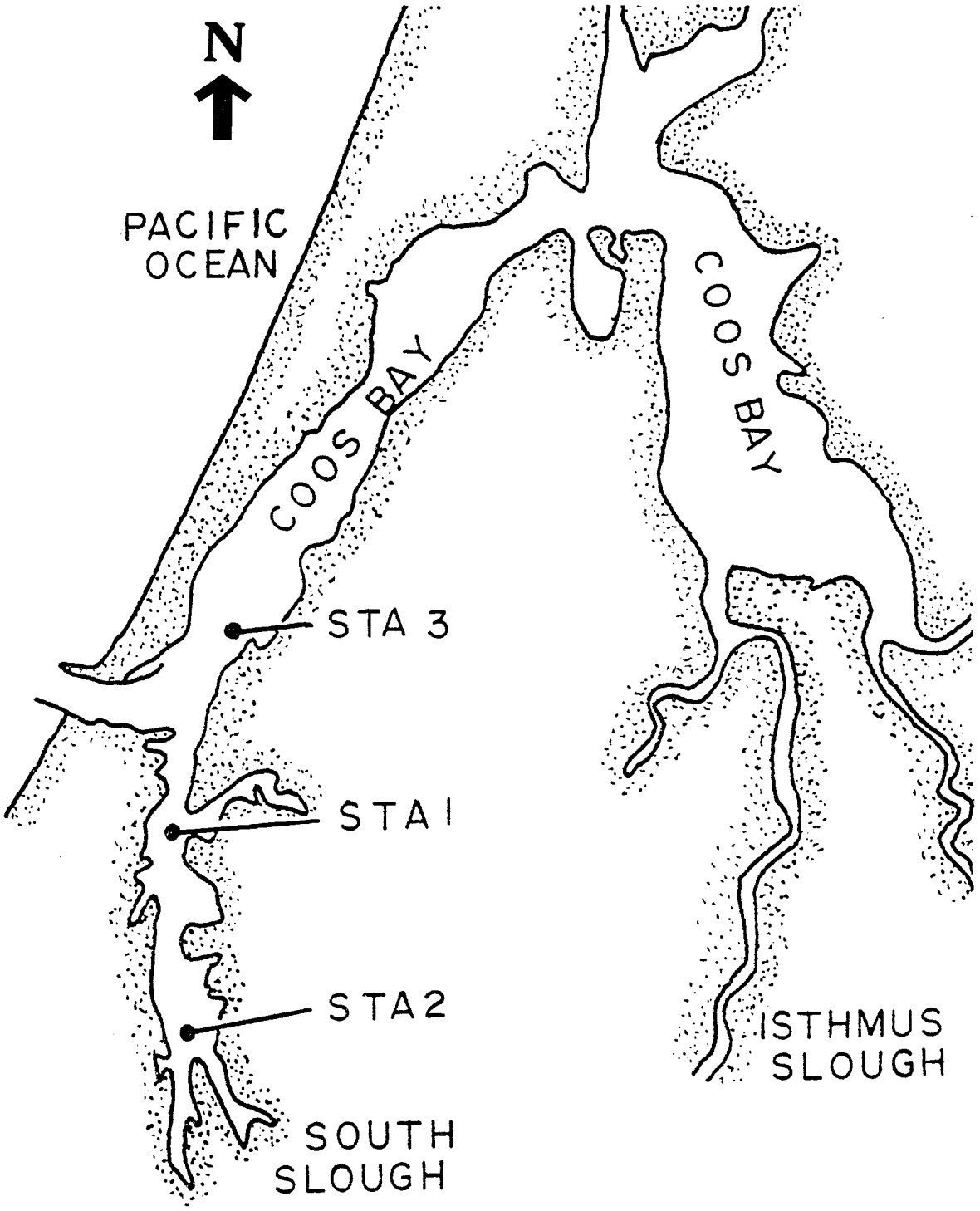

Fig. 1 Location of sand wave sampling Stations in Coos Bay, Oregon estuary { Lat 43° 22'N, Long 124° 18'W}

However, the speed of this motion is considered to be small compared with the speed of the free stream velocity and is neglected in the mathematical derivation. Mei(12) analysed steady flow with a periodic free surface over an impermeable stationary bottom also having a periodic shape. By considering the full nonlinear boundary conditions and by assuming the amplitude of the periodic bottom was of higher order in the perturbation parameter, he successfully removed the singularity present in the previous linearized studies and was able to determine the conditions required for the existence of a flat bottom. The key to this successful development was to assume that the bottom amplitude was of higher order in the perturbation parameter and that the speed of the free surface wave and the speed of the free stream flow were initially equal.

The major limitations of each of these models for measuring RST is that they only considered steady unidirectional flows and that the bottom boundaries are either impermeable or their motion must be determined empirically. The solution to the motion of an irregular, erodible and permeable bottom under oscillatory flows does not presently exist.

Lee(11) developed a stochastic theory and analysed the particle movement over a dune bed under unidirectional hydrodynamic flows. In his theory, Lee(11) assumed that the process of alternate erosion and deposition of sand grains is stochastic and that the rest periods and step lengths of the sand wave profile are Gamma distributed. The Gamma distribution for the rest periods and the step lengths is a two parameter positive semi-definite distribution {cf. Lee(11)}. Once the Gamma distributions are determined for sand wave data collected in an estuary, the mode of the distributions of the rest periods(T_m) and the step lengths(L_m) may be used to estimate the RST in the estuary. The celerity of the sand wave may be estimated by the relation $C = L_m/T_m$.

Hino(6) developed a spectral theory for the sand waves also in an unidirectional flow field. He derived the spatial and frequency spectra for sand waves based on a dimensional analysis. The wave number spectrum and the wave frequency spectrum are related by the

celerity of the sand wave profile in an estuary. The celerity of the sand wave profile may be estimated from the relation $C = f_m/k_m$, in which f_m is the peak frequency of the wave frequency spectrum and k_m is the peak wave number of the wave number spectrum of the sand waves. The frequency of the sand wave gives an estimate of the RST. The celerity of the sand wave may be used with the peak wave number of the sand wave number spectrum to estimate the RST.

The stochastic and spectral theories developed by Lee(11) and Hino(6), respectively, are for unidirectional hydrodynamic flows and were validated by these authors using data from laboratory experiments. An attempt was made in the present study to extend these theories to oscillatory flows using field data from an Oregon estuary. The theories developed by Lee(11) and Hino(6) are employed separately to estimate the RST from data collected from South Slough estuary, Coos Bay, Oregon.

2.0 STOCHASTIC ANALYSIS

In an application of the stochastic theory developed by Lee(11) to estimate the rate of sediment turnover, it is assumed that the movement of the sand particles on the sediment bed consists of a series of discrete steps or jumps separated by periods of no motion or rest. These discrete steps are termed "step lengths" and the periods of rest as "rest periods".

The spatial step lengths depend upon: 1) the geometrical shape of the spatial record of sand waves, $y_t(x)$; 2) the number of dune crests which the particle passes before it is deposited; and 3) the probability distribution of the elevations at which the particle is eroded and deposited. Longer step lengths are associated with longer dunes and with lower elevations at which the individual particle is eroded or deposited.

Similarly, the temporal rest periods depend upon: 1) the geometrical shape of the temporal record of sand waves; and 2) the elevation at which the particle is deposited. Shorter rest periods are associated with shorter dunes and with higher elevations at which the individual particle is deposited.

The probability distributions of these step lengths and rest periods may be estimated from measured sand wave records which are functions of space and time, respectively.

2.1 Step Length Distribution

The step length of a sand particle in a spatial sand wave record, $y_t(x)$, is defined {cf. Lee(11)} as the distance moved by the particle from its eroded position on the stoss side of a sand wave profile to its deposition position on the slip side of the sand dune profile. Fig. 2 adapted from Lee(11) is a definition sketch for the step length of a spatial sand wave record. In Fig. 2, the subscripts i, j and l for the step length represent the elevations of erosion, deposition and the number of dunes passed while in motion, respectively. Lee(11) in his stochastic theory assumed that the conditional step lengths could be represented by the two parameter Gamma probability

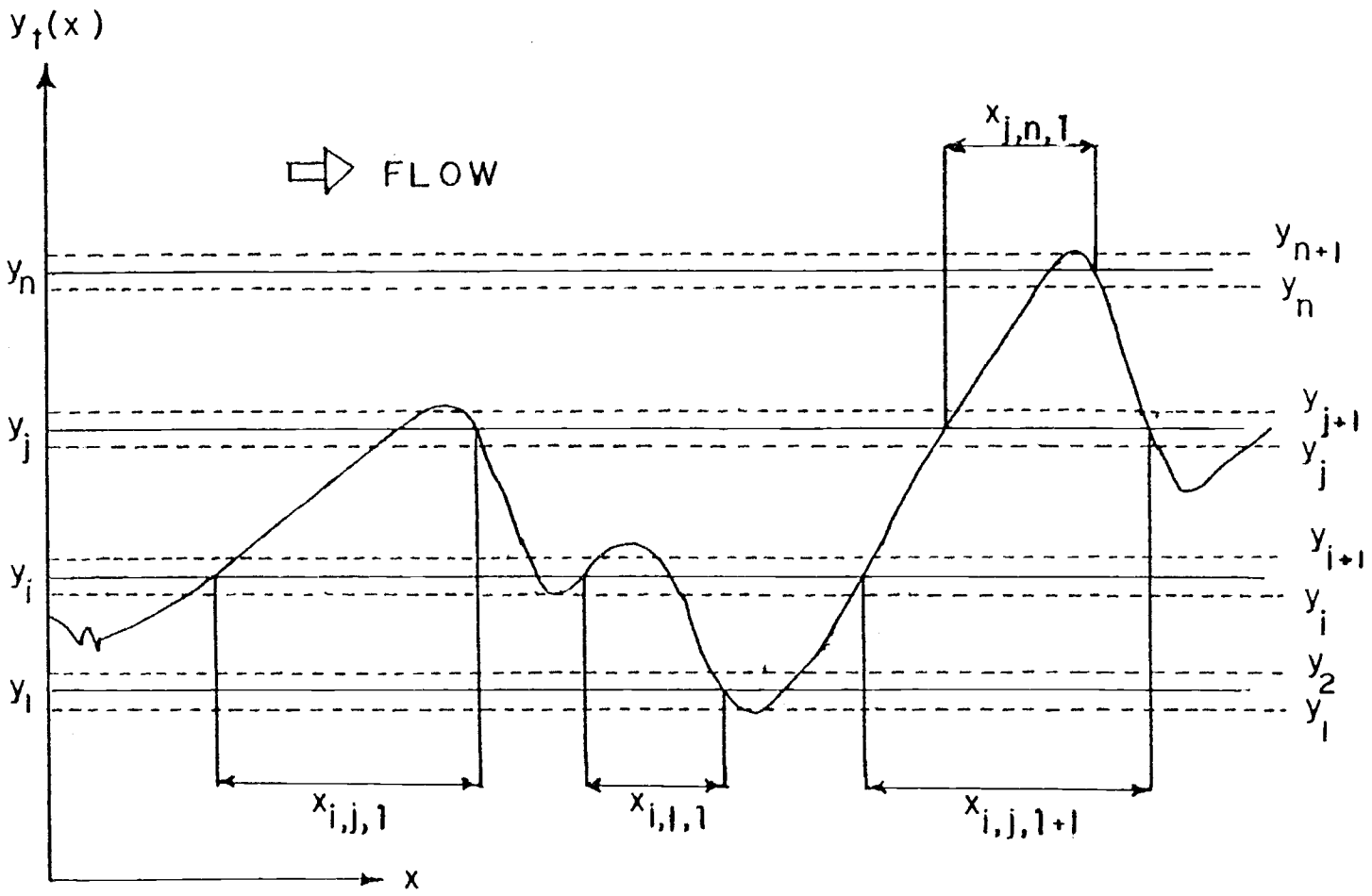

Fig. 2. Typical $y_t(x)$ record for the step length of a bed-load particle { cf. Lee(11)}

density function. This assumption for the conditional step lengths was verified by a Chi-square goodness-of-fit test using measured laboratory data {cf. Lee(11)}.

The two parameters required to construct the Gamma distribution are: 1) the scale, κ_1, and 2) shape, r_1, parameters. In order to estimate these parameters, it is necessary to estimate the mean and variance of step length distribution from measured spatial sand wave records. The mean and variance computed by Lee(11) are determined from

$$E\left[X|Y_E = y_i,\ Y_D = y_j\right] = \frac{1}{m_{i,j}} \sum_{l=1}^{m_{i,j}} x_{i,j,l} \tag{1a}$$

$$Var\left[X|Y_E = y_i,\ Y_D = y_j\right] =$$

$$\frac{1}{m_{i,j}} \sum_{l=1}^{m_{i,j}} (x_{i,j,l})^2 - \left[\frac{1}{m_{i,j}} \sum_{l=1}^{m_{i,j}} x_{i,j,l}\right]^2 \tag{1b}$$

in which $E\left[\cdot|\cdot\right]$ is an estimate of the conditional mean; $Var\left[\cdot|\cdot\right]$ is an estimate of the conditional variance; and $m_{i,j}$ represents the total number of bed forms in the sample of record in which the upstream side intersects the elevation y_i and the downstream side intersects the elevation y_j. In general, the term $m_{i,j}$ may be different for each combination of values of i and j(cf. Fig. 2). An estimate of the scale and shape parameters in terms of the conditional mean and variance are given by the following:

$$\kappa_1 = \frac{E\left[X|Y_E = y,\ Y_D = y'\right]}{Var\left[X|Y_E = y,\ Y_D = y'\right]} \tag{2a}$$

and

$$r_1 = E\left[X|Y_E = y,\ Y_D = y'\right]\kappa_1 \tag{2b}$$

in which κ_1 is the scale parameter and r_1 is the shape parameter.

After determining the scale and shape parameters, the step

length probability density distribution may be obtained according to

$$f_{X|Y_E,Y_D}(x|y,y') =$$

$$\frac{\kappa_1}{\Gamma(r_1)} (x\kappa_1)^{-1 + r_1} \exp\{-\kappa_1 x\} I_{(0,\infty)}(x) \qquad (3)$$

in which Y_E is the random variable describing the elevation of erosion; Y_D is the random variable describing the elevation of deposition; y and y' are the arguments for the random variables Y_E and Y_D; $\Gamma(r_1)$ is the Gamma function; and $I_{(0,\infty)}(x)$ is the Indicator function{ cf. Lee(11)}. It is assumed that all particles which are eroded from the stoss side of a dune will be deposited on the downstream side of the same dune wave.

2.2 Rest Period Distribution

The rest period of a sand particle in a temporal sand wave record, $y_x(t)$, is defined as the time lapse between the burial and re-exposure of the particle(cf. Fig. 3). These rest periods depend upon: 1) the geometrical shape of the temporal sand wave record and 2) the probability distribution of the elevation at which the particle is deposited. Like the step length, the probability density distribution of the conditional rest periods is approximated by the two parameter Gamma probability density function. The two parameters are the scale, κ_2, and shape, r_2, parameters. These parameters may again be estimated according to Lee(11) from

$$\kappa_2 = \frac{E\left[\bar{T}|Y_D = y'\right]}{Var\left[\bar{T}|Y_D = y'\right]} \qquad (4a)$$

and

$$r_2 = E\left[\bar{T}|Y_D = y'\right]\kappa_2 \qquad (4b)$$

in which $E[\cdot|\cdot]$ is an estimate of the conditional mean of the rest periods; $Var[\cdot|\cdot]$ is an estimate of the conditional variance of the rest periods; κ_2 is the scale parameter; r_2 is the shape parameter for the conditional rest period distribution. The estimates of the

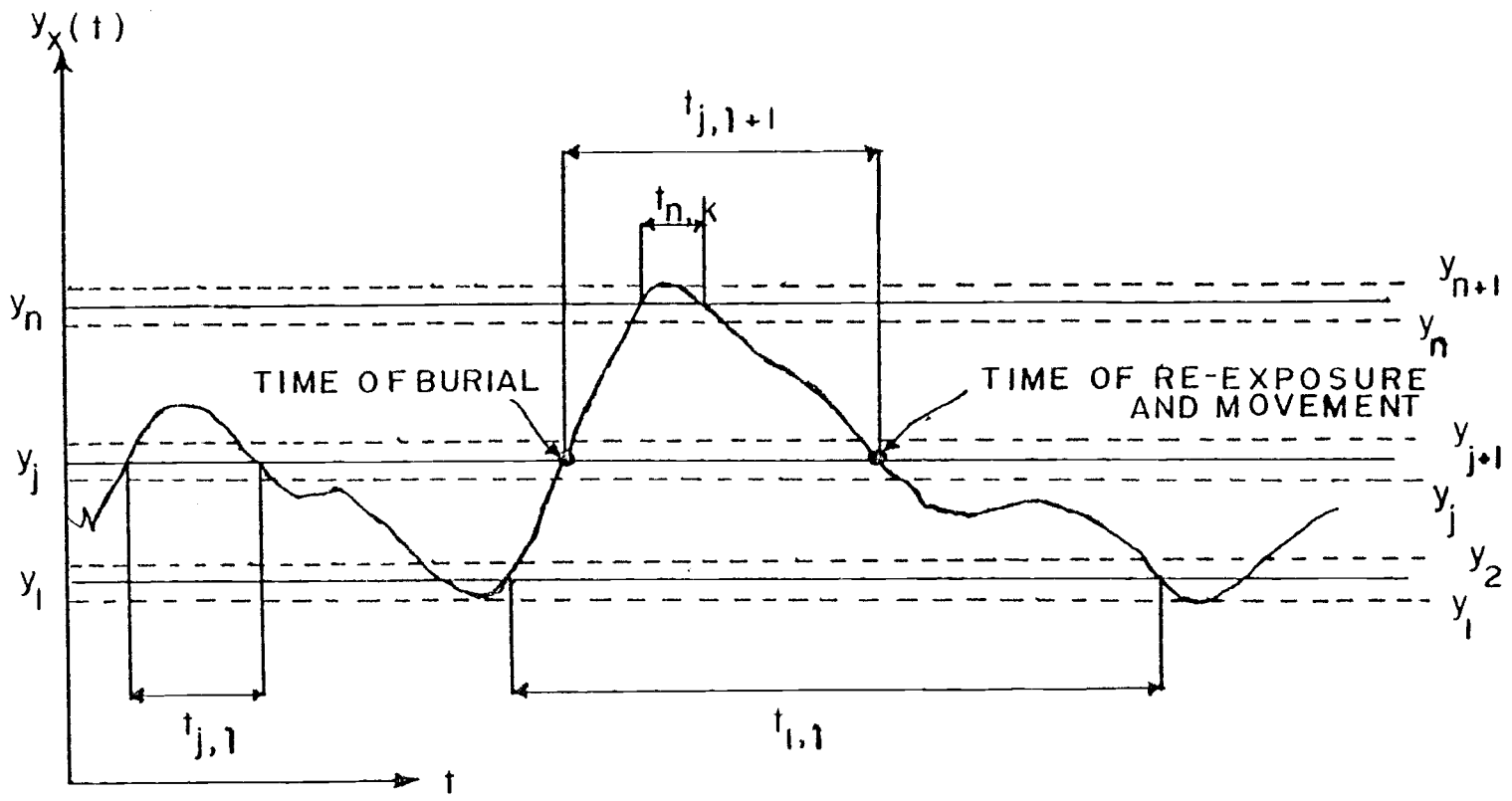

Fig. 3. Typical $y_x(t)$ record illustrating the conditional rest periods of a particle {cf. Lee(11)}

conditional mean and variance for the rest periods computed from measured temporal sand wave records which is given by Lee(11) are(cf. Fig. 3).

$$E\left[\bar{T}\middle| Y_D = y_j\right] = \frac{1}{m_{j,j}} \sum_{l=1}^{m_{j,j}} t_{j,l} \tag{5a}$$

$$Var\left[\bar{T}\middle| Y_D = y_j\right] = \frac{1}{m_{j,j}} \sum_{l=1}^{m_{j,j}} (t_{j,l})^2 - \left[\frac{1}{m_{j,j}} \sum_{l=1}^{m_{j,j}} t_{j,l}\right]^2 \tag{5b}$$

The probability density distribution of the conditional rest periods is given by

$$f_{\bar{T}|Y_D}(t|y') = \frac{\kappa_2}{\Gamma(r_2)} (\kappa_2 t)^{-1+r_2} \exp\{-\kappa_2 t\} I_{(0,\infty)}(t) \tag{6}$$

in which κ_2 is the scale parameter; r_2 is the shape parameter; $\Gamma(r_2)$ is the Gamma function; and $I_{(0,\infty)}(t)$ is the Indicator function.

The statistical equations given above may appear to be independent of flow parameters and bed material properties; however all of the statistics required for these equations must be estimated from a measured sand wave profile. Since the shape and rate of movement of sand waves are dependent upon the material properties of the benthic interface and the flow conditions, all of the equations are implicitly functions of the flow conditions and benthic material properties. Two key requirements used by Lee(11) are that; 1) the probability density distributions of the elevations of deposition and erosion must be Gaussian; and 2) a time series record of the migrating sand waves measured from a fixed location must be recorded. Profile measurements which deviate significantly from a Gaussian distribution are not considered to be valid for this type of stochastic analysis.

3.0 FOURIER ANALYSIS

An alternate method for estimating the rate of sediment turnover (RST) is by analysing the spectral representation of the sand wave profile. The random shape of the sand waves indicate that they could be represented by harmonic analysis consisting of a number of sinusoids of varying amplitudes and frequencies {cf. Cartwright(2), Crickmore and Lean(3), and Winant, et al.(17)}. For measurements of random sand waves recorded in space and time, the wave number spectrum may be related to the wave frequency spectrum by the celerity(or rate of translation) of the sand wave. The frequency of the sand wave gives an estimate of the RST. The celerity of the sand wave may be used with the peak of the sand wave number spectrum to estimate the RST.

Hino(6) derived a wave number and a wave frequency spectrum for the equilibrium subrange of sand waves. For fully developed or equilibrium sand waves, the slope of the sand bed profile may never exceed the angle of repose, ϕ, of the sand. This implies that a certain form for the large wave number spectrum exists in an equilibrium subrange in which the spectral form is governed predominantly be the angle of repose and the wave number. For low values of wave numbers, the sand waves are still growing and the law of equilibrium subrange fails due to an instability mechanism between the sand bed and flowing water.

3.1 Wave Number Spectrum

From a dimensional analysis for the equilibrium subrange, Hino(6) determined that the spectral density function for the elevation of the sand waves is of the form

$$S_{yy}(k) = \alpha(\phi)\, k^{-3} \quad ; \quad (k_o < k < d^{-1}) \tag{7}$$

in which k is the wave number in cycles per unit length; $\alpha(\phi)$ is a function of the angle of repose of a sand particle, which is considered to be a constant; d is the diameter of the sand particle; y is the elevation at any spatial position in the spatial sand wave record; and

k_o is the smallest value for the wave number of the sand wave field in which the interactional instability mechanisms are not important. From experimental data for unidirectional flow, Hino(6) found that an approximate value for k_o may be estimated from

$$k_o = 0.15/h \tag{8}$$

in which h is the depth of water in the channel.

3.2 Wave Frequency Spectrum

The wave frequency spectrum may be estimated from a temporal record of a sand wave profile. Hino(6) showed that within the equilibrium subrange, the frequency spectrum follows a "-3 power law" for higher frequencies and a "-2 power law" for frequencies which are slightly greater than the spectral peak frequency but which are less than the "-3 power law" frequencies. In the higher frequency region within the equilibrium subrange, the frequency spectrum for the sand wave profile is assumed from dimensional analyses to be given by

$$S_{yy}(f) = f(\Psi)\, V_*^2\, f^{-3} \quad ; \quad (f_1 < f < f_\infty) \tag{9}$$

in which f is the wave frequency in unit of cycles per unit time; $f(\Psi)$ is a function of Ψ, which is a nondimensional quantity related to the critical tractive force of the sand bed; V_* is the bed shear velocity; and f_1 and f_∞ are the lower and upper bounds, respectively, of the higher frequency region within the equilibrium subrange.

The wave number, k, and the wave frequency, f, of a sand wave are related by the wave celerity or rate of translation of the waveform according to

$$f = C(k)\, k \tag{10}$$

in which C is the celerity of the sand wave profile. The relationship between the frequency spectrum and the wave number spectrum may be determined by equating the areas under two differential distances Δk and Δf of the wave number and wave frequency spectral densities, respectively. Equating these differential areas, yields

$$S_{yy}(f) = S_{yy}(k) \frac{dk}{df} \tag{11}$$

In the lower wave number range for small values of the wave numbers below the spectral peak wave number and the equilibrium subrange, interactions between the sand waves and the water flowing over them become predominant as the sand waves are still growing. Within this lower wave number range the celerity must be considered to be a function of the wave number; i.e.,

$$C(k) \propto k \coth 2\pi kh \tag{12}$$

in which h is the depth of water in the estuary channel. Within the equilibrium subrange for wave numbers $k >> 1/2\pi h$, Eq. 12 may be approximated by

$$C(k) = \gamma k \tag{13}$$

in which γ is a dimensional constant with dimensions L^2/T. Substituting Eq. 13 into Eq. 10 and taking derivatives on both sides, we get

$$\frac{dk}{df} = \frac{1}{2\gamma k} \tag{14}$$

The equilibrium subrange of the wave number spectrum must extend to wave numbers lower than for the equilibrium subrange of frequency spectrum {Hino(6)}. The equation for the frequency spectrum for this relatively lower frequency region within the equilibrium subrange may now be obtained by substituting Eqs. 7 and 14 into Eq. 11;

$$S_{yy}(f) = \frac{1}{2}\alpha(\phi)\gamma f^{-2} \quad ; \quad (f_o < f < f_1) \tag{15}$$

in which f_o is the lowest value for the wave frequency in the wave spectrum, which corresponds to the lowest wave number, k_o.

In summary, within the equilibrium subrange for the wave number spectrum, Hino(6) concludes that there must be two different frequency regions for the wave frequency spectrum. He gives the following two forms for the wave frequency spectrum within this equilibrium subrange:

$$\{\text{-3 power law}\}: \quad S_{yy}(f) = f(\Psi)\, V_*^2\, f^{-3} \quad ; \quad (f_1 < f < f_\infty) \qquad (9)$$

$$\{\text{-2 power law}\}: \quad S_{yy}(f) = \frac{1}{2}\,\alpha(\phi)\gamma\, f^{-2} \quad ; \quad (f_0 < f < f_1) \qquad (14)$$

The key to the successful application of this method for estimating RST lies in determining the appropriate constant of proportionality, γ, and the angle of repose function, $\alpha(\phi)$.

It may be observed that an inconsistency exists in the derivation of the wave frequency spectrum by Hino(6). He showed that within the equilibrium subrange, the frequency spectrum follows a "-3 power law" for higher frequencies and a "-2 power law" for frequencies which are slightly greater than the spectral peak frequency but which are less than the "-3 power law" frequencies. This indicates that two dispersion relationships are required for the sand waves within the equilibrium subrange. Since the wave frequency spectrum is of prime importance in the estimation of RST, a "-3 power law" was derived for the entire wave frequency equilibrium subrange which corresponds to the wave number equilibrium subrange. The key to the successful derivation of a "-3 power law" for the entire wave frequency equilibrium subrange lies in the selection of a transformation between wave numbers and wave frequencies which contains the same dimensional parameters used in the dimensional analyses for the spectrum. It may be shown that the square of the bed shear velocity is directly proportional to the square of the bed shear velocity in a channel {cf. Cartwright(2)}. Since the celerity of the sand bed is either related to the stream velocity {cf. Kennedy(7, 8)} or depends on the shear velocity{cf. Hino(6), Gradowczyk(4)}, it may be assumed that the celerity of the sand wave profile is a function of the bed shear velocity. This transformation and the derivation of the wave frequency spectrum are shown in Appendix I.

If a transformation between wave numbers and wave frequencies is known, the RST may be estimated from the peak frequency f_m of the frequency spectrum calculated from the wave number spectrum since the peak of the frequency spectrum may be estimated by Eq. 11. This may reduce the requirement to obtain a time series for sand waves in order to estimate the wave frequency spectrum. A schematic representation for

obtaining the RST from a sand wave number spectrum is shown in Appendix II. An additional method for estimating RST is also given in Appendix III.

4.0 DATA COLLECTION

4.1 Experimental Apparatus

For the stochastic and the Fourier analyses, measurements of sand wave elevations as a function of space, $y_t(x)$ {cf. Fig. 2}, in South Slough, Coos Bay, Oregon estuary, were recorded by mechanical and acoustic profilers, respectively.

The mechanical profiler was constructed from two wooden beams of rectangular cross section approximately 3.6 m long. Two aluminum I beam sections were mounted vertically to each end of these wooden beams. Approximately 180 holes were drilled through the long dimension of the rectangular cross section of each of the wooden beams at intervals of approximately 2.0 cm. Bicycle spokes which were fitted with a piece of small plastic tubing approximately 1.0 cm long were inserted through these holes and coated with wax to prevent undesired movement under gravity. This piece of small plastic tubing also marked the elevation of the sand profile below the level mounted on each wooden beam. A schematic representation of this mechanical profiler is shown in Fig. 4 in which the components are identified by the following numbers: 1) an aluminum pipe parallel to the cross section of the sand wave profile; 2) a wooden beam parallel to the direction of the sand wave profile; 3) screw anchors to secure the aluminum pipe; 4) concrete block anchors to secure the wooden beams; 5) a wooden frame(3 x 5 cm in cross section) which is required to connect the two wooden beams to the aluminum pipe; and 6) a level mounted on each wooden beam.

The mechanical profiler was placed on the sandy bottom of the estuary by a pair of divers operating from a shallow draft inflatable boat during periods of slack tide. The mechanical profiler was placed parallel to the direction of the flow field at a convenient elevation (usually about 60 cm) above the wavy bottom of the estuary. The spatial sand wave records were obtained during two sampling periods between July 26 - 28, 1975 and between September 22 - 24, 1975. The sampling location(STA 1) is shown in Fig. 1. These data are summarized in Table 1. Since the records were measured during periods of slack tide(i.e., no flow), the time necessary to make the sand bed profile

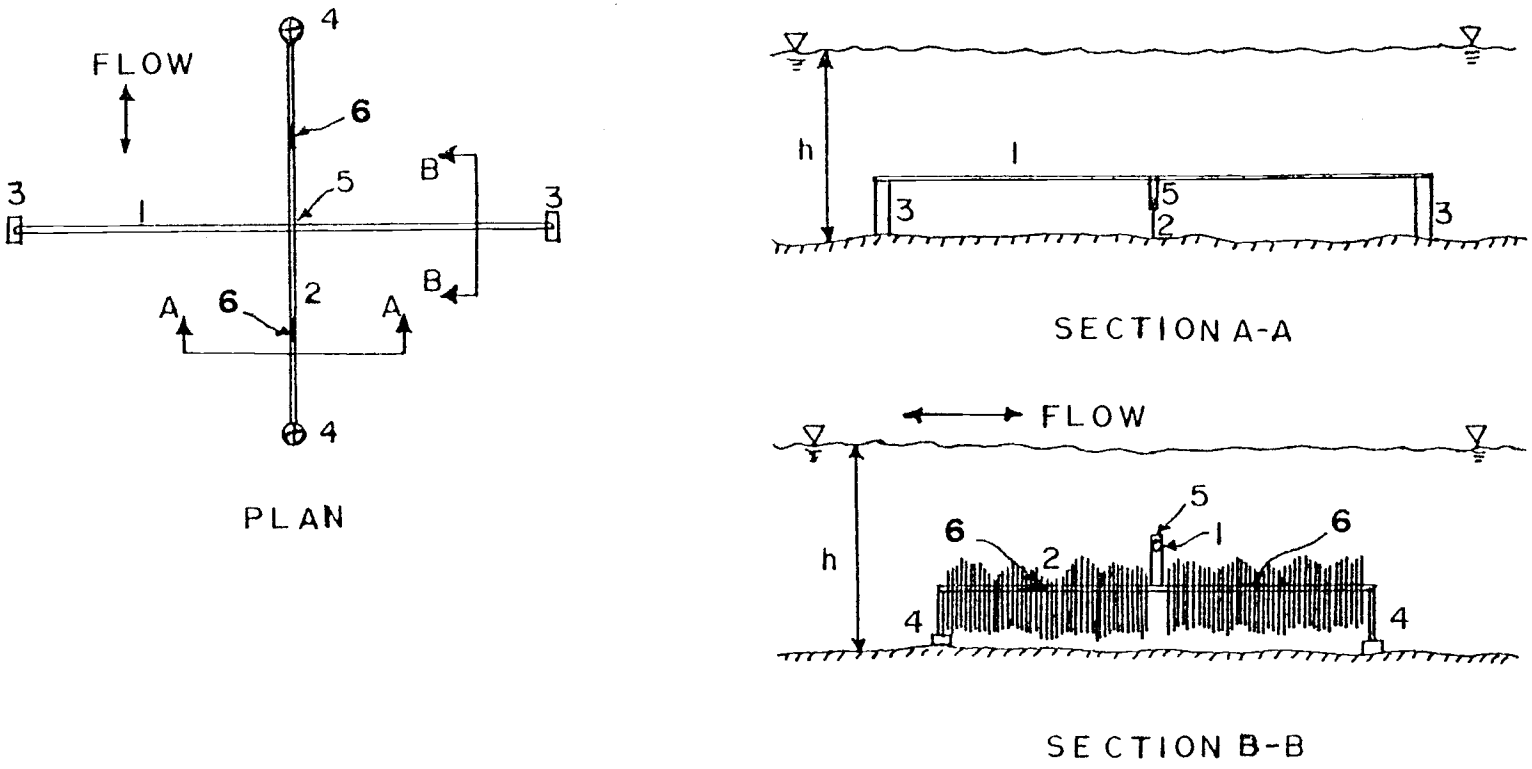

Fig. 4. Schematic of the Mechanical Sand Wave Profiler in place

Table 1. Summary of Data from Mechanical Profiler

Record (1)	Date (2)	Time (3)	Tide in meters (4)	Previous Current (5)	Remarks (6)
AB-I	08-26-'75	1410-1500	1.983(High)	Flood	Good Visibility
AB-II	08-28-'75	1020-1115	0.702(Low)	Ebb	Good Visibility
AB-III	09-22-'75	1340-1500	2.074(High)	Flood	Good Visibility
AB-IV	09-23-'75	0810-0940	0.580(Low)	Ebb	Poor Visibility
AB-V	09-23-'75	1400-1450	2.074(High)	Flood	Poor Visibility
AB-VI	09-24-'75	0830-1000	0.671(Low)	Ebb	Poor Visibility
AB-VII	09-24-'75	1430-1600	2.580(High)	Flood	Good Visibility

measurements may be assumed to be small compared to the time scale of sediment motion and a record of $y_t(x)$ was obtained.

For the Fourier analysis, the sand wave profiles were recorded by means of a sonic profiler during a two day period, December 18-19, 1975. A long steel pipe was mounted vertically to the side of a boat. The sonic profiler was secured to the underwater end of the steel pipe approximately 0.8 m above the sand bed. The sonic data were recorded directly on FM magnetic tape in analog form by a FM tape recorder aboard the boat. The sonic sampling locations(STA 1, 2, 3) are shown in Fig. 1.

Five buoys were implanted and the distances between these buoys were measured by means of a range finder(transit type) on the shore. The buoys were taut and anchored to the bottom of the estuary so that their drift was minimum. Before recording the sonic data on a magnetic tape at each station, the boat was driven very slowly along the course of the buoys and the time of travel between the buoys was recorded by a stop watch. The speed of the boat was then computed by dividing the known distances between the buoys by the recorded time required for the boat to cover these distances at each station. The speed of the boat was approximately equal to 0.5 m/sec. It was attempted to maintain the speed of the boat at each station at approximately a constant value of 0.5 m/sec during each measurement of data recording operation. Two data recordings at STA 1; four data recordings at STA 2; and one data recording at STA 3 were recorded during the two day data recording period. All of these seven runs of data recorded at the three locations(STA 1, 2, 3) are tabulated in Table 2.

In order to measure the <u>in situ</u> length of the sand wave records from the magnetic tape, the passing of each buoy by the sampling boat was demarcated by voice on the same channel of the magnetic tape as the sonic data. These boat speed estimates are required for the data analysis which is explained in detail in Chapter V.

The pulse rate for the sound waves from the sonic profiler was 1/30 second. The rate of data sampling is high compared to the speed at which the boat was moving(approximately 0.5 m/sec) to insure that no sand wave elevation was missed from the recordings. In order to

eliminate vertical disturbances to the boat, data were collected when the water surface disturbances were minimum. In order to maintain sufficient draft for the sampling boat, data were collected only during the slack period of high tide

Table 2. Summary of Data from Sonic Profiler

Record No. (1)	Date (2)	Length in meters (3)	Length in seconds (4)	Variance in $meters^2$ (5)	$H_{r.m.s}$ in meters (6)	Δk in $meters^{-1}$ (7)	k_o in $meters^{-1}$ (8)	Sampling Location (9)
1	12-18-'75	91.09	236	0.0113	0.30	0.011	0.075	STA 1
2	12-18-'75	127.53	471	0.1348	1.04	0.008	0.075	STA 1
3	12-19-'75	211.34	675	0.0615	0.70	0.005	0.038	STA 2
4	12-19-'75	211.34	400	0.0337	0.52	0.005	0.038	STA 2
5	12-19-'75	211.34	402	0.0654	0.72	0.005	0.038	STA 2
6	12-19-'75	216.02	540	0.0427	0.58	0.005	0.038	STA 2
7	12-19-'75	45.81	270	0.2382	1.38	0.022	0.017	STA 3

5.0 DATA ANALYSES

5.1 Stochastic Analysis

To check the Gaussian property of the elevations of erosion and deposition for the measured sand wave records collected in South Slough estuary, Coos Bay, Oregon, the records were averaged about the mean and standardized(i.e., normalized) by the standard deviation of each record. A constant dimensionless class interval of 0.4 {Benjamin and Cornell(1)} was adopted and the number of class intervals for the elevations of deposition and erosion was determined by knowing the maximum and minimum elevations in the record. Histograms for two sample standardized records are shown in Fig. 5. It may be seen that these histograms for the elevations of deposition and erosion of record AB-I and AB-II are not Gaussian.

To determine the parameters for the step length distribution, a standardized $y_t(x)$ record was digitized with a constant class interval, $\Delta y = 0.4$, and the step lengths($x_{i,j,l}$) were determined at different combinations of elevations of erosion(i) and deposition(j). The scale and shape parameters required for the step length distribution for a sample record AB-I were estimated from Eqs. 2a and 2b and are summarized in Table 3. The conditional step length distribution from Table 3 is selected for a constant standardized elevation of deposition and erosion, $Y_{SD} = Y_{SE} = -1.4$. The Gamma probability density distribution for the step length at the standardized elevations, $Y_{SD} = Y_{SE} = -1.4$, is shown in Fig. 6. The mode of the distribution is approximately 3.0 cm. This low statistic reflects a high frequency bias in the stochastic method which results from the assumption that a particle only passes one sand dune.

5.2 Fourier Analysis

The sonic sand wave data which were recorded by a sonic profiler on a FM magnetic tape were copied on an analog strip chart for visual observation of the sand wave records. The total length of each run was computed both in meters and in seconds. The length of the run in meters was computed by recording by voice on the magnetic tape

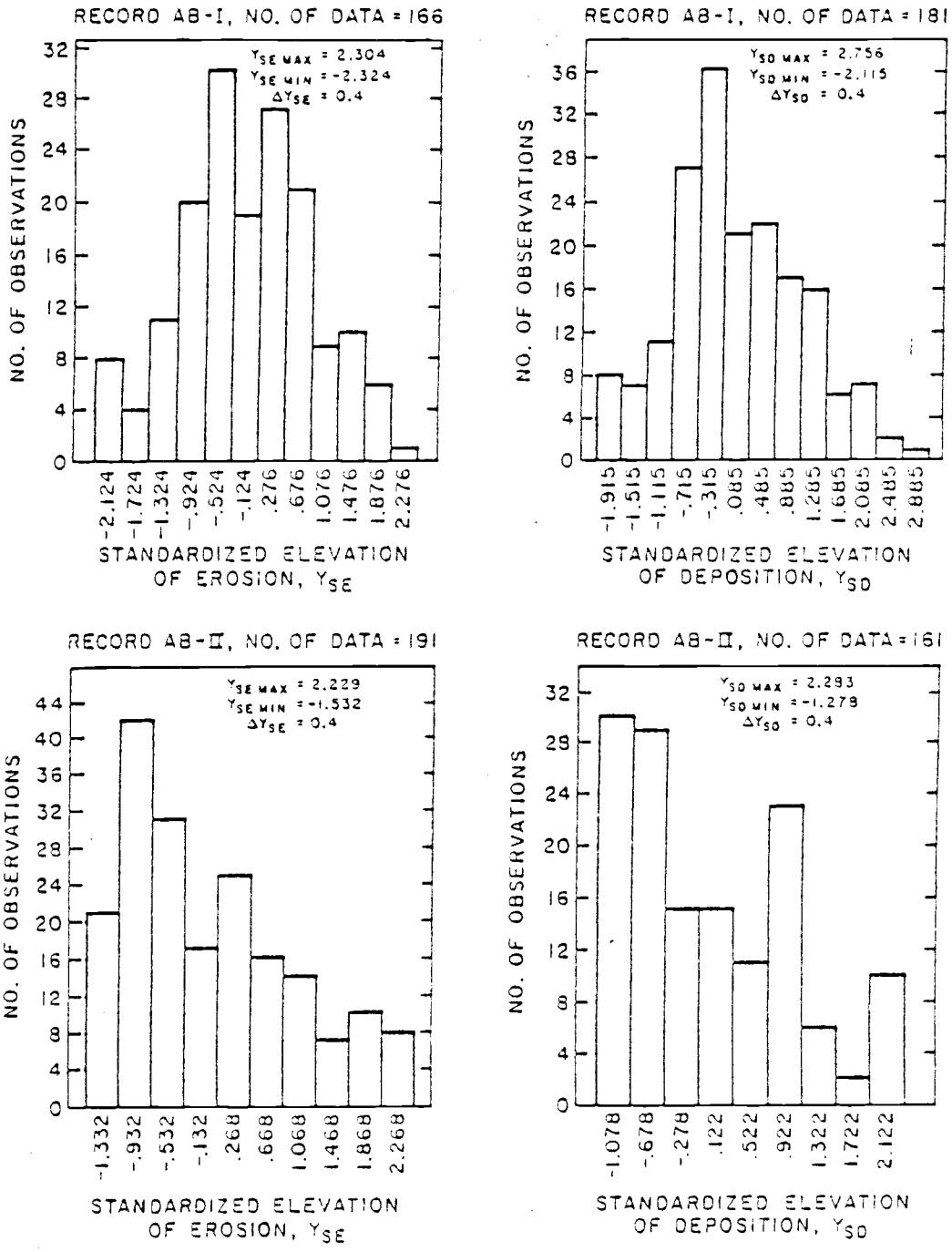

Fig. 5 Histograms of the standardized elevations of deposition/ erosion for record AB-I from a mechanical profiler

Table 3. Scale and Shape parameters of Gamma density function for conditional step length distribution for Record AB-I

Y_{SD} / Y_{SE}	-1.4 (1)	-1.0 (2)	-0.6 (3)	-0.2 (4)	0.2 (5)	0.6 (6)	1.0 (7)	1.4 (8)	1.8 (9)
-1.4	0.839 (3.568)	---	---	---	---	---	---	---	---
-1.0	---	0.785 (3.802)	0.061 (1.072)	---	---	---	---	---	---
-0.6	---	0.191 (2.504)	0.101 (1.131)	0.167 (2.873)	0.356 (5.758)	---	---	---	---
-0.2	---	0.420 (14.272)	0.973 (23.352)	4.988 (71.825)	1.194 (10.551)	---	---	---	---
0.2	---	---	0.363 (6.334)	0.363 (3.245)	0.436 (1.780)	0.160 (1.428)	0.200 (1.362)	---	---
0.6	---	---	---	---	0.419 (2.726)	0.856 (3.369)	0.134 (1.087)	---	---
1.0	---	---	---	---	---	---	0.147 (0.861)	0.343 (2.662)	---
1.4	---	---	---	---	---	---	---	3.492 (11.524)	1.488 (6.398)
1.8	---	---	---	---	---	---	---	---	2.000 (16.000)

Note: Scale parameter = κ_1 { cm^{-1} }
(Shape parameter)= r_1 { Non-dimensional }

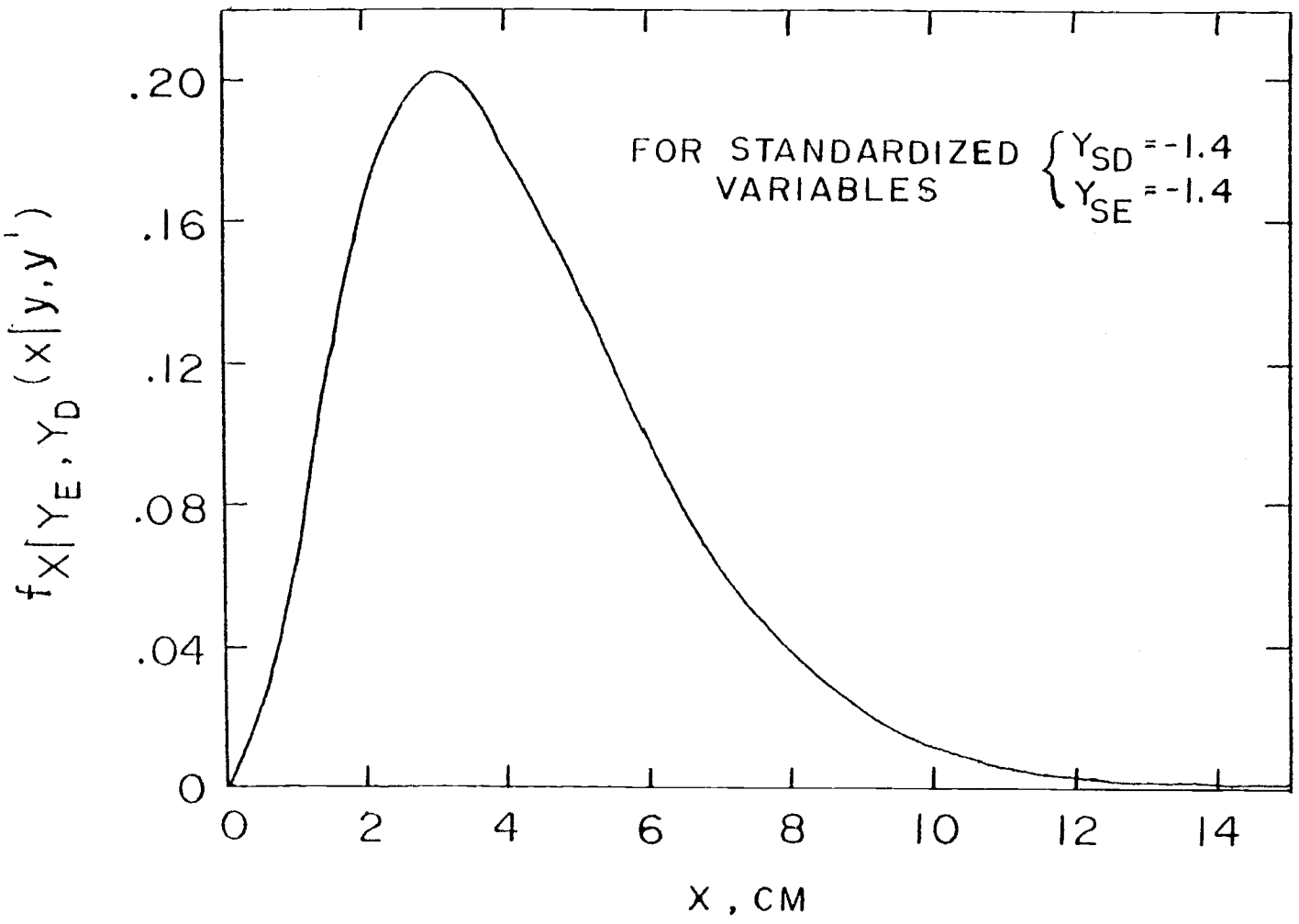

Fig. 6. Conditional Step Length Distribution for Record AB-I

when the sampling boat passed the positions of the buoys. The length in seconds of each record was computed by using a stop watch. The tape recorder was operated at the same speed at which data were recorded. The elapsed time between the start and the end of each record gave the total length of the record in seconds. The total length of the sand wave records in seconds was required in order to digitize the sand wave record by an analog to digital converter through a PDP 11 E10 minicomputer. The length of the sand wave records in time is also used to estimate the average speed of the boat by dividing the total length of the course between buoys in meters by the total time of the record.

The spatial resolution, Δx, of each sand wave record was computed by multiplying the tangent of the sonic profiler beam angle(5°) and the vertical height of the sonic profiler above the sand bed(approximately 0.8 m). The spatial resolution, Δx, computed from the above method was approximately equal to 0.15 m. This spatial resolution was then compared with the horizontal distance between two consecutive sound waves to insure that it is greater than the horizontal distance between two consecutive sound waves. This horizontal distance between two consecutive sound waves was computed by multiplying the average speed of the boat and the rate at which the sound waves were sent. Once the spatial resolution of each record was determined, the total number of digitizing values, N, may be computed from the relation

$$N \geq L/\Delta x \tag{16}$$

in which N is the total number of digitizing values and L is the total length of the sand wave profile in meters. The digitizing time, Δt, was then computed from the relation

$$\Delta t = T/N \tag{17}$$

in which T is the total time of the record in seconds obtained from the analog magnetic tape. Data recorded by the sonic profiler were digitized at the time intervals determined from Eq. 16 by an analog to digital converter through a PDP 11 E10 minicomputer.

The spatial sand wave data recorded by the sonic profiler were

first linearly detrended and then the amplitude spectra were estimated by an integer finite Fourier transform(FFT) algorithm of base two. The amplitude spectra for some of these sand waves which were recorded at 3 different locations in Coos Bay estuary are shown in Figs. 7 to 12. The variance, the r.m.s wave height and the equal discrete wave number interval are summarized in Table 2.

The amplitude spectra of the sand wave records from the South Slough estuary, Coos Bay, Oregon(Figs. 7 to 11) demonstrate two important points. First, the energy(variance of the time series) of the spectra are relatively low(e.g., min $H_{r.m.s}$ = 0.3 m for record No. 1) Second, most of the energy is contained in the fundamental harmonic component. This indicates that the dynamic migration of these sand waves is a slow, low energy phenomenon and the sand bed is a slowly undulating boundary.

For the sand wave records from the South Slough estuary(record Nos. 1 to 6; Figs. 7 to 11), the maximum spectral amplitudes are found at wave numbers which lie below the smallest wave number of the equilibrium subrange given by Hino(6) for unidirectional flow in the laboratory. This shows that the sand waves in the South Slough estuary are still growing. In the South Slough estuary the root mean square sand wave height, $H_{r.m.s}$, varies from 0.30 m to 1.04 m.

In contrast, sand waves in the Coos Bay main channel have higher energy which are dispersed over a wider band of wave numbers; however, the fundamental harmonic still contains the most energy. This is due to the stronger tidal velocities which are augmented by the ship propeller disturbances in the main channel. Since this spectral comparison is only a visual comparison, the spectral band width parameter which provides an estimate of the width of the wave frequency spectrum {cf. Kinsman(9)}, should be computed from the wave frequency spectrum in order to obtain the dispersion of the spectrum about the spectral peak. The sand wave frequency spectrum may be obtained from the wave number spectrum by using a theoretical or empirical transformation between the wave numbers and the wave frequencies. A flow chart for obtaining RST from a wave number spectrum using a dispersion transformation is given in Appendix II.

For the sand wave record from the Coos Bay main channel(record No. 7; Fig. 12), the wave number of the maximum spectral amplitude falls very close to the minimum wave number value for the equilibrium subrange given by Hino(6). In Fig. 12, we note that the minimum wave number value for the equilibrium subrange, k_o, given by Hino(6) is slightly less than the first harmonic component. This demonstrates that some care must be taken when digitizing a record in order that the value for the minimum wave number for the equilibrium subrange, k_o, will be much greater than the fundamental harmonic component. For example, if we assume that k_o will appear in nth harmonic(i.e., $k_o = n\,\Delta k$; $n > 1$), the equal discrete wave number interval, Δk, may be estimated from Eq. 8 according to

$$\Delta k = \frac{0.15}{n\,h} \tag{18}$$

in which h is the depth of water in the estuary channel. Knowing Δk and the spatial resolution, Δx, from the data acquisition, the total number of digitized values, N, may be computed from:

$$N = (\Delta x\,\Delta k)^{-1} \tag{19}$$

For Coos Bay main channel, if we assume that k_o will appear in the 5th harmonic, the equal discrete wave number interval, Δk, may be estimated from Eq. 18. As a result, we get $\Delta k = 0.0033\ m^{-1}$. Substituting this equal discrete wave number interval in to Eq. 19, we get $N = 2048$. This shows that for the Coos Bay main channel, the spatial sand wave record should have been digitized with at least 2048 values instead of 1024 which was used in the present analysis in order that k_o will be much greater than the fundamental harmonic component.

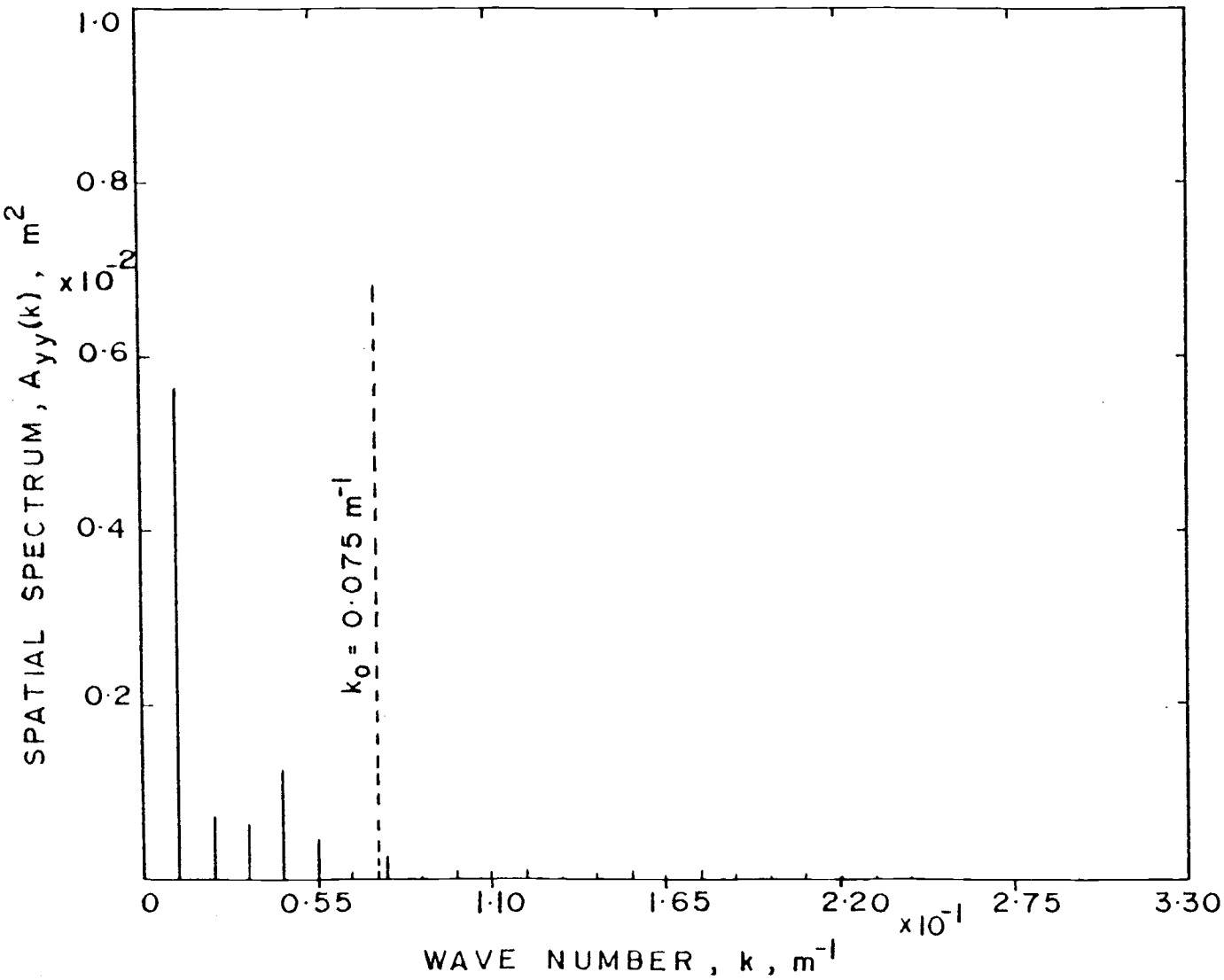

Fig. 7. Sand wave amplitude spectrum for Record No. 1 {V = 0.0113 m^2, Δk = 0.011 m^{-1}}

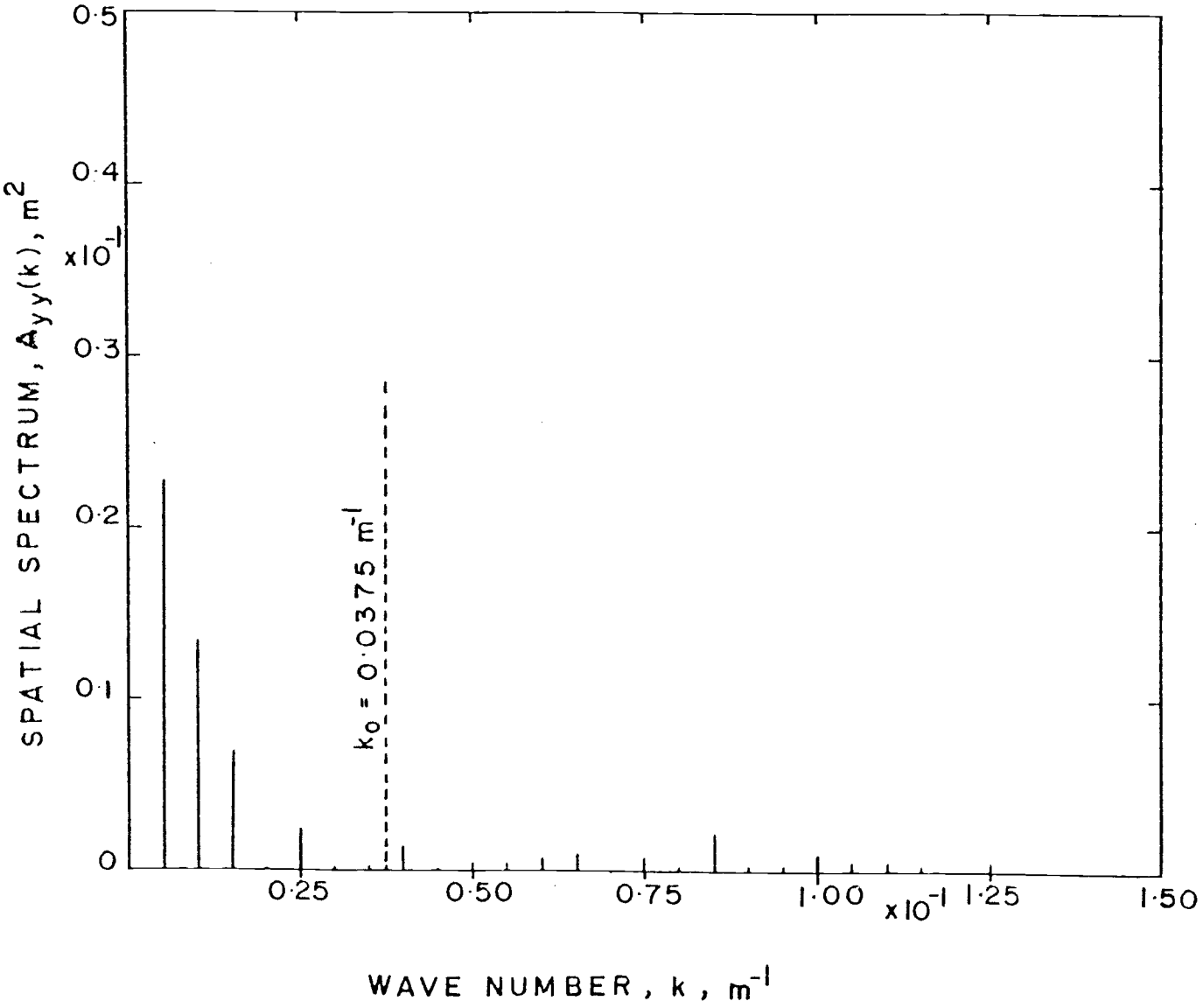

Fig. 8. Sand wave amplitude spectrum for Record No. 3 { V = 0.0615 m^2, Δk = 0.005 m^{-1} }

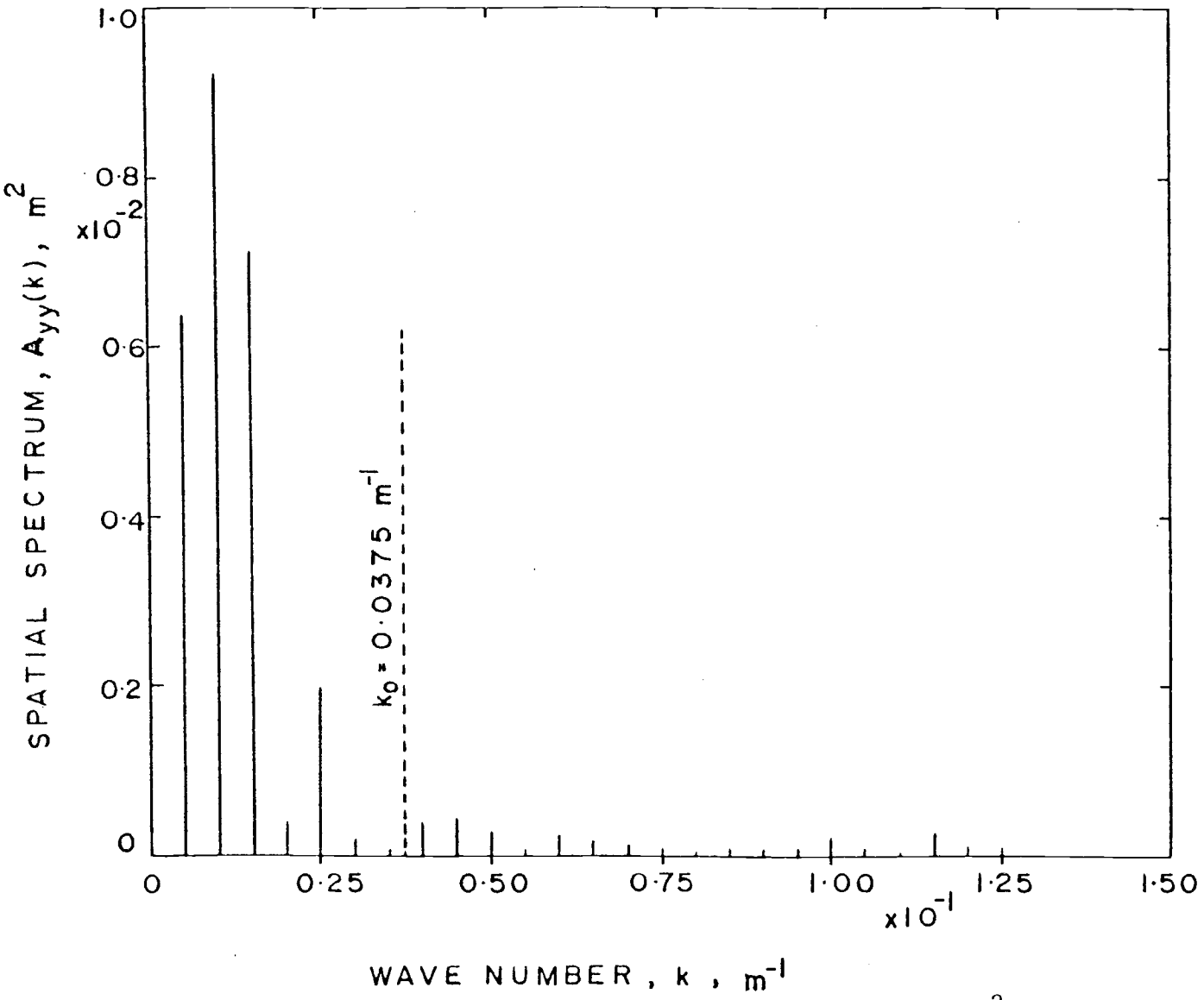

Fig. 9. Sand wave amplitude spectrum for Record No. 4 { $V = 0.0337\ m^2$, $\Delta k = 0.005\ m^{-1}$ }

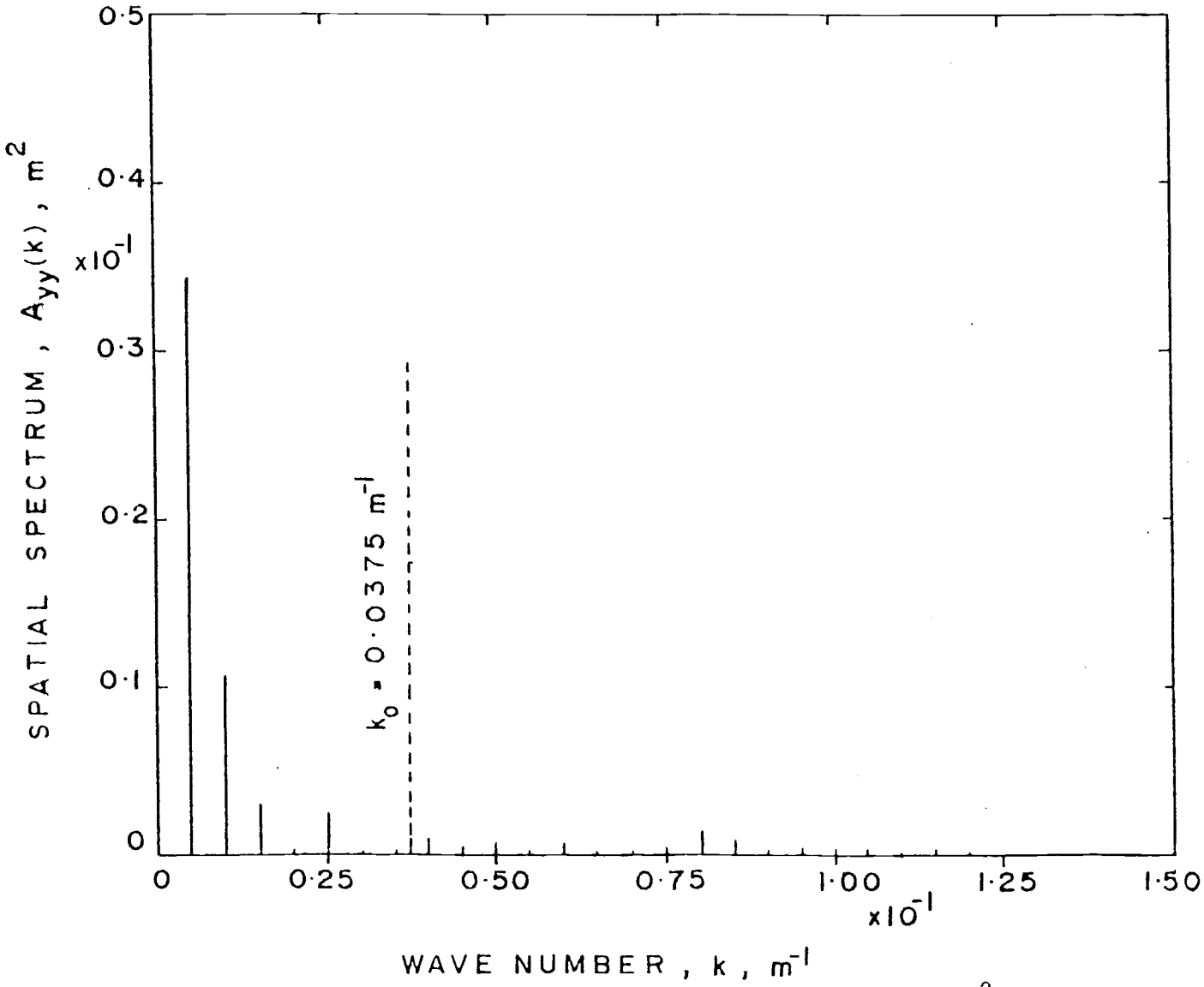

Fig. 10. Sand wave amplitude spectrum for Record No. 5 { V = 0.0654 m^2, Δk = 0.005 m^{-1} }

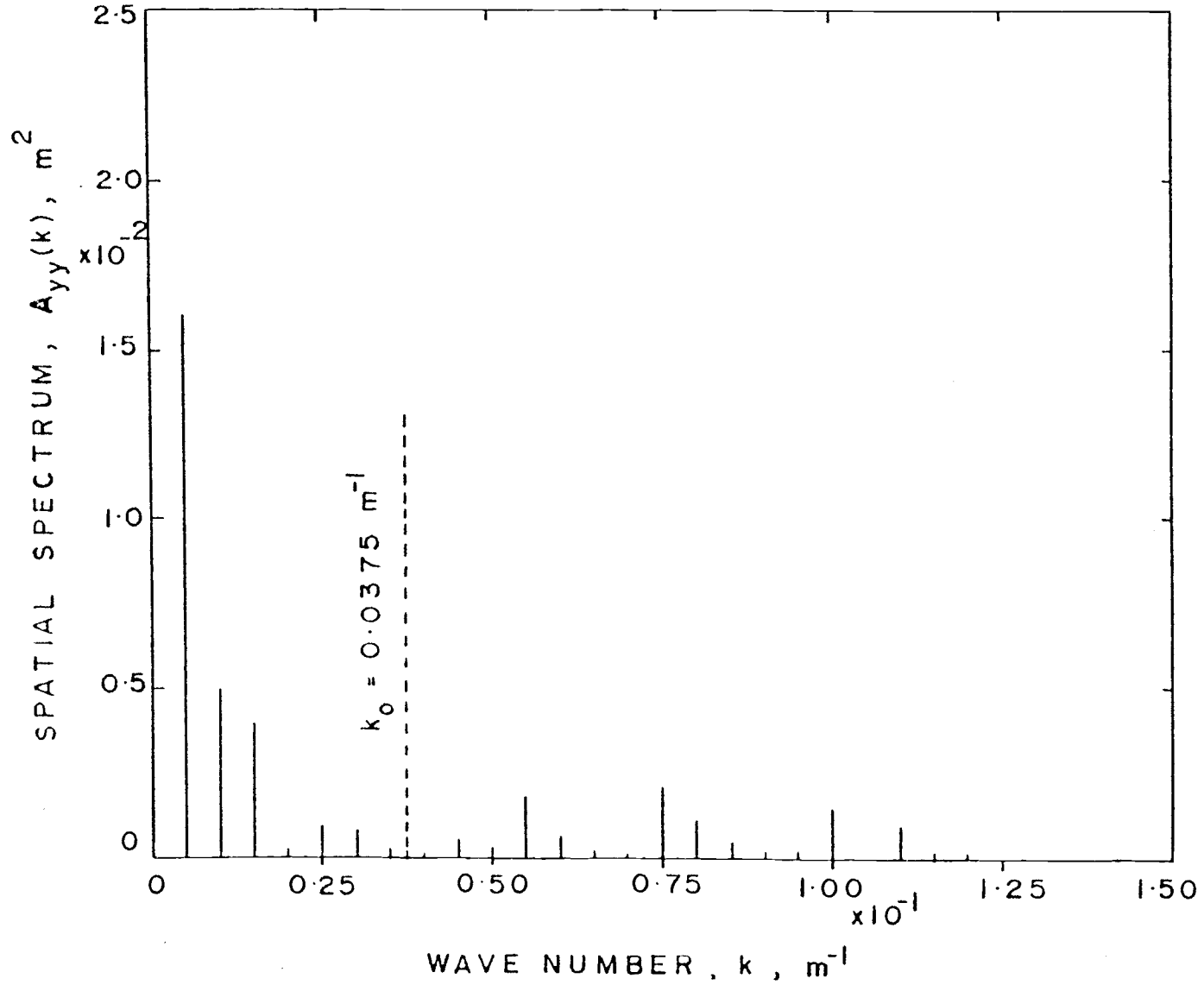

Fig. 11. Sand wave amplitude spectrum for Record No. 6 { $V = 0.0427\ m^2$, $\Delta k = 0.005\ m^{-1}$ }

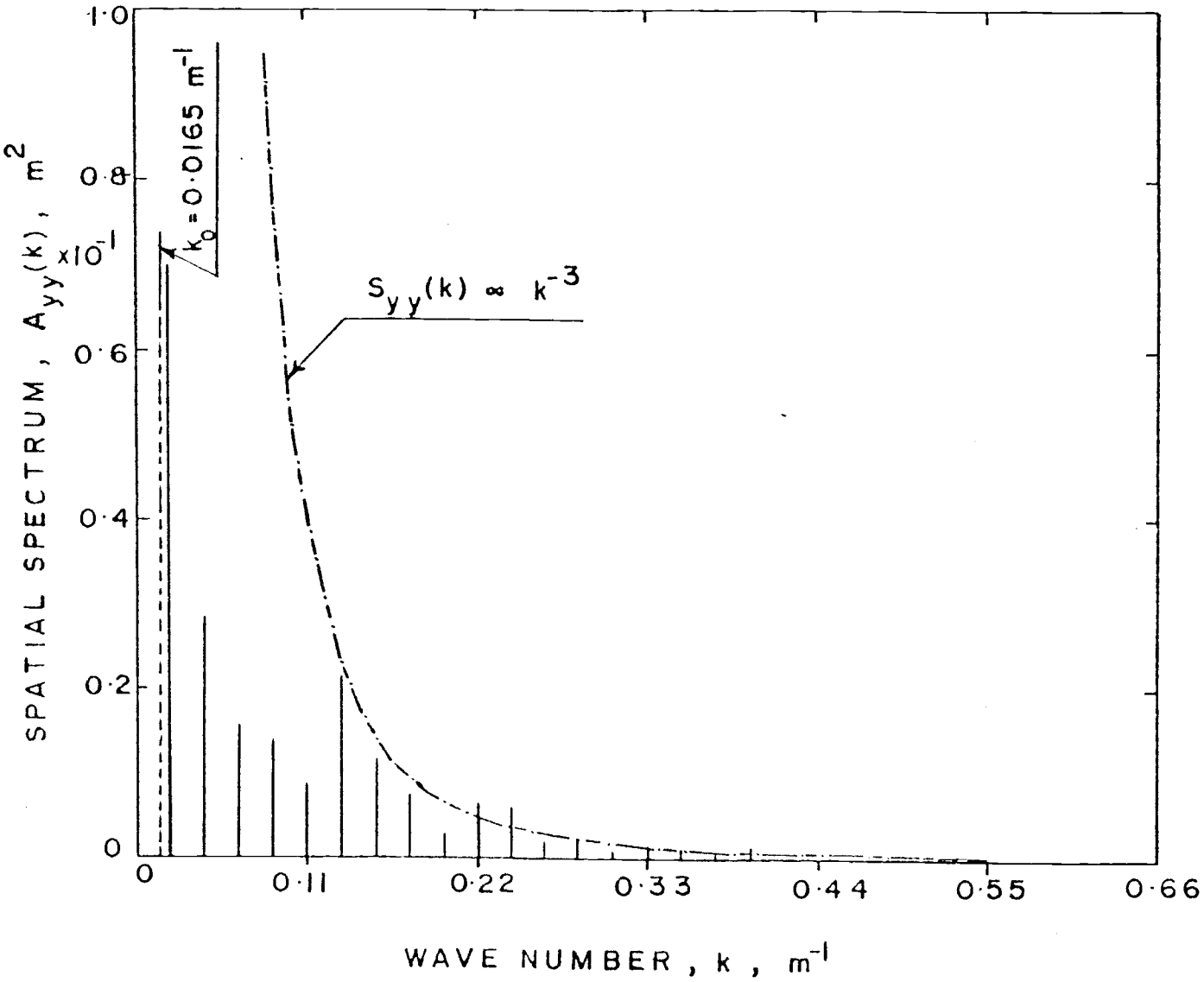

Fig. 12. Sand wave amplitude spectrum for Record No. 7 { V = 0.2382 m^2, Δk = 0.022 m^{-1} }

6.0 SUMMARY AND CONCLUSIONS

In order to estimate the RST in South Slough estuary, Coos Bay, Oregon, sand wave data were collected by two methods of measurement for sand wave analyses by two theories. For the stochastic analysis, data were collected by a mechanical profiler; while for the Fourier analysis, data were collected by a sonic profiler.

6.1 Stochastic Analysis

In the stochastic analysis, discrete data collected by the mechanical profiler were normalized by the standard deviation of the elevations of the sand wave profile. Histograms of the elevations of deposition and erosion were plotted in order to obtain the probability distributions for the elevations of deposition and erosion of the sand wave profile. To check the validity of the Gaussian distribution for the elevations of deposition and erosion, a sand wave record for the elevations of deposition and erosion was digitized at a dimensionless class intervals of, $\Delta y = 0.4$. It was observed visually from these histograms that the Gaussian property was not satisfied. However, the stochastic analysis developed by Lee(11) for unidirectional flow was continued for one set of data only in an attempt to extend his analysis to the oscillatory flow in the Coos Bay estuary. The two parameters required to construct the Gamma probability distribution for step lengths from the measured data were estimated according to the methods outlined by Lee(11) for unidirectional flow and the distribution was obtained for record AB-I. The mode of the distribution for the step lengths was found to be approximately 3 cm for record AB-I. This low modal statistic from the distribution for the step lengths indicates that a sand particle which is eroded from the stoss side of a sand wave at an elevation would move only a very short distance before it is deposited at the same elevation on the slip side. This shows that these sand waves are small ripples and they are still in the initial stage of their growth. This is due to the weak hydrodynamic influence in the South Slough estuary. The distributions for the step lengths were not estimated for the remaining data because the

the histograms for the elevations of deposition and erosion did not demonstrate a Gaussian distribution. In addition, the time series sand wave records were not recorded and, consequently, no estimate of the mode of the Gamma distribution for the rest period could be computed. This modal statistic for the rest period is required in order to estimate the RST.

The sediment turnover which is caused by the erosion and deposition of sand particles is due to the hydrodynamic influences on the sand bed. Since the hydrodynamic influences on the sand bed are very weak in the South Slough estuary, the sediment turnover in the South Slough estuary may occur due to the collapse of the fully grown sand waves. Since these sand waves(record AB-I) are still in the initial stage, it may not be possible to estimate the RST in the South Slough estuary, Coos Bay, Oregon by the stochastic method outlined by Lee(11).

To estimate the RST in an estuary by the stochastic method developed by Lee(11), it is also necessary to obtain the mode of the distribution for the rest periods. The distribution for the rest periods was not obtained since temporal sand wave records were not recorded for analysis. A great deal of difficulty is involved in obtaining this time dependent record since the profile sensor must be introduced into the flow field without significantly disturbing the flow. Furthermore, if the oscillatory motion of the wave like benthic interface is a slowly varying time function, the profile sensor must either be protected against long term mechanical and biological degradation or repositioned exactly at the same location at relatively short time intervals over a number of oscillatory cycles. This second requirement for repositioning involves expensive navigational positioning systems.

Based on the analysis presented above, it may be concluded that it is presently not possible to apply the stochastic theory developed by Lee(11) to estimate RST under oscillatory flow in an estuary. This is due, in part to the assumption that the discrete jumps taken by the eroding sand particles are restricted to the event that only one wave crest or sand dune is passed during each jump. For a wide banded sand wave spectrum, this assumption biases the statistical rest periods

which must be estimated from the mode of the rest period Gamma distribution towards the high frequency range because the proportion of the nagative maxima increases steadily with the relative width of the spectrum. The proportion of the negative maxima is defined as the ratio of the negative maxima to the sum of the negative maxima plus the positive maxima. In addition, the stochastic analysis developed by Lee(11) is some what tedious and time consuming to apply since the analytical development for the stochastic method does not include a dispersion relationship for transformations between time and space, and therefore, both temporal and spatial data records must be obtained.

Future research in the stochastic theory should concentrate on incorporating the oscillatory time dependence of the flow field into analysis. It is also recommended that the assumption that a particle only passes one sand dune should be reexamined with regard to oscillatory flows.

6.2 Fourier Analysis

For the Fourier analysis, the sonic data of sand wave elevations were recorded on a magnetic tape in analog form by a sonic profiler in the South Slough estuary, Coos Bay, Oregon. These data were digitized by using an analog to digital converter in a PDP 11 E10 minicomputer and the wave number amplitude spectra were estimated by an integer finite Fourier transform(FFT) algorithm.

From the FFT analysis, it may be observed that most of the energy(variance of the time series) is contained in the fundamental harmonic component of the sand wave spectra for the data recorded in the South Slough estuary. This indicates that in the South Slough estuary the sand bed is a slowly undulating boundary. It may also be noted that the wave numbers of the maximum spectral amplitudes lie below the smallest wave number of the equilibrium subrange computed by Hino(6) for unidirectional flow in the laboratory. It is also observed that the energy(variance) of the sand wave spectra in the South Slough estuary are relatively low compared to the energy of the sand wave spectrum in the main channel. In the South Slough estuary

the root mean square sand wave height, $H_{r.m.s}$, varies from 0.30 m to 1.04 m compared to $H_{r.m.s}$ = 1.38 m for the Coos Bay main channel. From the equilibrium subrange of the wave number spectra(Figs. 6 to 11), it may be noted that the sand waves in the South Slough estuary are still growing since the wave number of the maximum spectral amplitude is very much smaller than the smallest wave number of the equilibrium subrange computed by Hino(6). Also, no measurable energy exist in the equilibrium subrange. This is due to the weak tidal velocities in the shallower South Slough estuary.

For the sand wave record from the Coos Bay main channel(record No. 7; Fig. 12), the wave number of the maximum spectral amplitude falls very close to the equilibrium subrange computed by Hino(6). In the main channel the root mean square sand wave height is found to be 1.38 m.

For the Coos Bay main channel, the energy is dispersed over a wider band of wave numbers but the fundamental harmonic still contains the most energy. This is due to the stronger tidal velocities which are augmented by the ship propeller disturbances in the main channel. Since the spectral comparison is only a visual comparison, the spectral band width parameter which provides an estimate of the width of the wave frequency spectrum {cf. Kinsman(9)}, should be computed from the wave frequency spectrum in order to obtain the dispersion of the spectrum about the spectral peak. The sand wave frequency spectrum may be obtained from the wave number spectrum by using a dispersion transformation between the wave numbers and the wave frequencies.

The digitizing interval for FFT in the above analysis was estimated from the spatial resolution of the data acquisition only. In order to obtain the minimum wave number value for the equilibrium subrange, k_o, in higher harmonic, the digitizing interval for FFT should also be determined from the equal discrete wave number, Δk, which was estimated from the minimum wave number value for the equilibrium subrange.

Based on the spectral analysis, it is concluded that the spectral analysis method may be more readily adapted to estimate the RST in an

estuary under oscillatory flows. This is due to the fact that in this method of analysis only a spatial sand wave record is required to estimate RST since a dispersion transformation for sand waves may be incorporated in order to eliminate the difficulty of recording a time series record for sand waves in an estuary. Once the wave frequency spectrum is obtained from the wave number spectrum by using the dispersion transformation, the RST may be estimated from the peak frequency of the wave frequency spectrum.

In summary, based on both the stochastic and the Fourier analyses, it may be concluded that the Fourier analysis is relatively simpler and requires only a spatial sand wave record together with the dispersion transformation to estimate RST in an estuary; whereas the stochastic analysis requires both a spatial and temporal sand wave records in order to estimate RST in an estuary.

REFERENCES

1. Benjamin, J. R., and Cornell, C. A., Probability, Statistics, and Decision for Civil Engineers, McGraw-Hill Book Co., New York, 1970, pp. 1-17.
2. Cartwright, D. E., "On Submarine Sand-Waves and Tidal Lee-Waves," Proceedings of Royal Society of London, Series A, Vol. 253, London, England, 1959, pp. 218-240.
3. Crickmore, M. J., and Lean, G. H., "The Measurement of Sand Transport by Means of Radioactive Tracers," Proceedings of Royal Society of London, Series A, Vol. 266, London, England, 1962, pp. 402-421.
4. Gradowczyk, M. H., "Wave Propagation and Boundary Instability in Erodible-bed Channels," Journal of Fluid Mechanics, Vol. 33, 1968, pp. 93-112.
5. Graf, W. H., Hydraulics of Sediment Transport, McGraw-Hill Book Co., New York, 1971, pp. 273-303.
6. Hino, M., "Equilibrium-range Spectra of Sand Waves Formed by Flowing Water," Journal of Fluid Mechanics, Vol. 34, 1968, pp. 565-573.
7. Kennedy, J. F., "The Mechanics of Dunes and Antidunes in Erodible-bed Channels," Journal of Fluid Mechanics, Vol. 16, 1963, pp. 521-544.
8. Kennedy, J. F., "The Formation of Sediment Ripples, Dunes and Anti-Dunes," in Annual Review of Fluid Mechanics, Annual Reviews, Inc., Palo Alto, California, 1969, pp. 147-168.
9. Kinsman, B., Wind Waves, Prentice-Hall, Inc., Englewood Cliffs, New Jersey, 1965, pp. 51-112, 325-361, 427-487.
10. Lamb, H., Hydrodynamics, 6th Ed., Dover Publications, New York, 1945, pp. 398-410.
11. Lee, B. K., "Stochastic Analysis of Particle Movement Over a Dune Bed," thesis presented to Colorado State University, at Fort Collins, Colorado, in 1973, in partial fulfillment of the requirements for the degree of Doctor of Philosophy.
12. Mei, C. C., "Steady Free Surface Flow Over Wavy Bed," Journal of the Engineering Mechanics Division, ASCE, Vol. 95, No. EM6,

REFERENCES(continued)

Proc. Paper 6967, Dec., 1969, pp. 1393-1402.

13. Milne-Thompson, L. M., Theoretical Hydrodynamics, 5th Ed., The MacMillan Co., New York, 1969, p. 444.
14. Raudkivi, A. J., Loose Boundary Hydraulics, Pergamon Press, New York, 1967, pp. 175-221.
15. Reynolds, A. J., "Waves on an Erodible Bed of an Open Channel," Journal of Fluid Mechanics, Vol. 22, 1965, pp. 113-133.
16. Wehausen, J. V., "Surface Waves," in Handbuch der Physik, Vol. 9, Springer-Verlag, 1960, pp. 569-570.
17. Winant, C. D., Inman, D. L., and Nordstrom, C. E., "Description of Seasonal Beach Changes Using Empirical Eigenfunctions," Journal of Geophysical Research, Vol. 80, 1975, No. 15, pp. 1979-1986.

APPENDICES

APPENDIX I

Gradowczyk(4) has shown that the celerity of the sand wave profile is proportional to the bed shear velocity. Previous analysis of surface gravity waves { cf. Hino(6)} has been consistent in the equilibrium subrange. This may be due to the consistency of dimensional parameters used in the wave frequency spectral equation and the wave number dispersion equation. Therefore, a transformation between wave numbers and wave frequencies may be assumed to be given by

$$C^2 = \gamma V_*^2 \tag{20}$$

in which C is the sand wave celerity; V_* is the bed shear velocity; and γ is a dimensionless constant. Note that the constant, γ, in the dispersion equation assumed by Hino(6) is a dimensional quantity having the dimensions of L^2/T.

Substituting Eq. 20 into Eq. 10 and differentiating, we obtain

$$\frac{dk}{df} = \frac{1}{\gamma^{\frac{1}{2}} V_*} \tag{21}$$

Combining Eqs. 21, 7, and 11, the wave frequency equilibrium subrange becomes

$$S_{yy}(f) = \alpha(\phi)\, \gamma^2\, V_*^2\, f^{-3} \quad ; \quad (f_o < f < f_\infty) \tag{22}$$

The lowest frequency which corresponds to the lowest wave number, k_o, in the equilibrium subrange given by Hino(6) is identified as "f_o".

The upper wave number range in the equilibrium subrange is assumed by Hino(6) to be given by

$$k = d^{-1} \tag{23}$$

in which d is the diameter of the sand particle. Substituting Eq. 23 into Eq. 20, the upper frequency limit, f_∞, may be found to be

$$f_\infty = \gamma^{\frac{1}{2}} V_* d^{-1} \tag{24}$$

Hence, a "-3 power law" for the entire sand wave frequency equilibrium subrange may be given as

$$S_{yy}(f) = \alpha(\phi)\ \gamma^2\ V_*^2\ f^{-3} \quad ; \quad (f_o < f < \gamma^{\frac{1}{2}}\ V_*\ d^{-1}) \qquad (25)$$

APPENDIX II

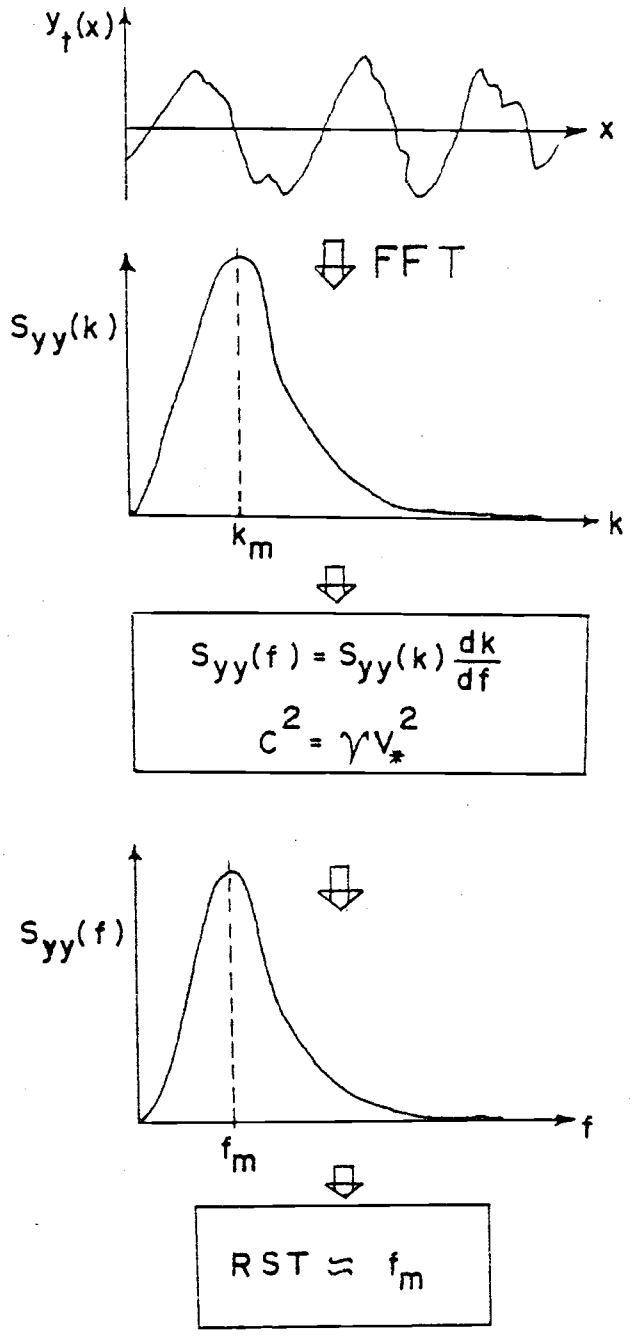

Flow Chart for Estimating RST from wave number spectrum by Dispersion Transformation

APPENDIX III

An Additional Method for Estimating RST

It is also possible to estimate the celerity of the sand wave profile from the shear stress at the sand bed. If the velocity of the water in a channel is known, the shear stress at the sand bed may be estimated by estimating the drag force on the bed due to the flow of water in a channel.

The shear stress at the sand bed due to the flowing water is given by:

$$\tau = \beta \rho_w \omega^2 \tag{26}$$

in which τ is the shear stress at the sand bed; β is the drag coefficient; ρ_w is the density of water; and ω is the velocity of water in a channel. The shear stress at the sand bed may also be written as a function of the celerity of the sand bed, i.e.,

$$\tau = \beta \rho_s C^2 \tag{27}$$

in which ρ_s is the density of the sand particles; and C is the celerity of the sand bed.

To satisfy the dynamic boundary condition at the sand bed, the shear stress due to the flowing water should be equal to that due to the motion of the sand bed. Therefore, equating Eqs. 26 and 27, we get

$$C = \left(\frac{\rho_w}{\rho_s}\right)^{\frac{1}{2}} \omega \tag{28}$$

Knowing the flow of water in a channel, it may be possible to estimate the celerity of the sand bed from the continuity of shear stress. Using this celerity and a spatial sand wave record, it may be possible to estimate RST in an estuary.